Hindawi
Advances in Materials Science and Engineering
Volume 2018, Article ID 7175083, 9 pages
https://doi.org/10.1155/2018/7175083

Research Article

On the Modelling of Thermal Aging through Neutron Irradiation and Annealing

Boris Margolin[1], **Elena Yurchenko**[1], **Vera Potapova**[1] **and Valery Pechenkin**[2]

[1]*Nuclear Research Center "Kurchatov Institute"–Central Research Institute of Structural Materials "Prometey", Shpalernaya St., 49, 191015 Saint-Petersburg, Russia*
[2]*State Science Center–"Institute for Physics and Power Engineering", Bondarenko Sq. 1, 249020 Obninsk, Kaluga Region, Russia*

Correspondence should be addressed to Boris Margolin; margolinbz@yandex.ru

Received 31 October 2017; Revised 14 May 2018; Accepted 23 May 2018; Published 2 July 2018

Academic Editor: Pavel Lejcek

A new method predicting long-term thermal embrittlement of steel caused by P segregation is verified. The method is based on the results of impact strength or fracture toughness tests using specimens after relatively short-term neutron irradiation followed by annealing. 2Cr–Ni–Mo–V steel used in reactor pressure vessels of WWER-1000 type is investigated in four conditions: initial condition, after thermal aging, after neutron irradiation, and postirradiation annealing. The results of impact strength and tensile tests and SEM investigation are presented. The brittle fracture features are considered for different material conditions. Calculative estimation on neutron irradiation effect on P diffusion in steels is carried out. Experimental data are reported which confirm an intense P diffusion acceleration under neutron irradiation.

1. Introduction

Thermal aging is the dominant degradation mechanism proceeding in unirradiated component (e.g., nozzle shell) materials for WWER-type reactor pressure vessels (RPVs). Therefore, thermal aging of RPV materials during NPP operation should be predicted for an adequate structural integrity assessment of unirradiated RPV components. The WWER-1000 RPV operation temperature is 290–320°C. Lifetime for this type reactor is planed to be extended at least up to 60 years.

The prediction of thermal aging of RPV materials for 60 years is rather a complicated task. The point is that thermal aging of surveillance specimen sets proceeds at the same temperature as that of RPVs. Therefore, surveillance specimen test results are relevant only to the current condition of RPV materials (for the moment of taking out surveillance specimens). Further material aging process can be predicted only through extrapolation.

Long-term prediction of thermal aging of materials is usually based on the test results of specimens subjected to accelerated aging at temperatures higher than the RPV operation temperatures. Such an approach results from the assumption that the material aging is controlled only by diffusion processes, and the equilibrium concentration of a diffusing element on some sinks (e.g., on grain boundaries) is temperature-independent. For this case, long-term prediction of thermal aging is usually based on the Arrhenius equation [1–3]. In particular, the Hollomon parameter which determines the degree of material aging depending on exposure time and temperature is one of the most commonly used [4, 5].

The phosphorus content for unirradiated RPV component materials is up to 0.020% as per relevant technical specifications. High P contents are known to result in thermal embrittlement of metal due to P segregation at grain boundaries (GBs). The equilibrium grain boundary P concentration is a temperature-dependent parameter, decreasing with increase of temperature [2, 3, 6]. Therefore, the prediction of P aging for the WWER-type RPV materials on the basis of the results of accelerated aging at higher temperatures and the Hollomon parameter application can be inadequate and nonconservative.

The above gave impetus to the development of a new method predicting "phosphorus" embrittlement of RPV steels. This new method was reported in the paper [7].

Its main idea consists in accelerating P segregation processes by neutron irradiation at a temperature corresponding to that of RPV operation (T_{oper}). Unlike the acceleration of P segregation processes only due to increasing a temperature, neutron irradiation hardly affects equilibrium P segregation [8, 9]. At the same time, irradiation accelerates the kinetics of P segregation through radiation-enhanced diffusion [8–22]. This acceleration results from the fact that the P diffusion coefficient increases considerably through the generation of point defects under irradiation [8, 9, 11–14]. As can be seen, the mechanism of forming P segregations is the general mechanism of metal embrittlement under thermal aging and neutron irradiation. The P diffuses towards different intragranular interphase boundaries (e.g., interphase carbide-matrix boundaries) as well as towards GBs and forms local segregations [3, 10, 19, 23–25]. As should be noted that P segregation does not lead to material hardening as P segregates mainly on GBs and on various intragranular barriers for dislocations that exist before irradiation (e.g., carbides). It means that P does not form new additional barriers for moving dislocations. At the same time, P segregations decrease the strength of interphase boundaries (e.g., carbide-matrix boundaries) or grain boundaries that makes the initiation of cleavage microcracks or intergranular brittle microcracks easier and, as a consequence, leads to material embrittlement [3, 19, 26–29]. Since the above mechanism of material embrittlement does not result in its hardening, such an embrittlement mechanism is referred to as a nonhardening mechanism [26, 27, 30].

It is necessary to note also that P also segregates on dislocation loops and precipitations [19, 31, 32]. Such segregations hardly affect material hardening [10].

The proposed method [7] consists in determining material embrittlement after the following two-stage treatment. At the first stage, accelerated neutron irradiation for short time with high neutron flux is conducted at $T = T_{oper}$, which hardly changes the value of equilibrium P segregation and, at the same time, accelerates the formation of P segregations due to radiation-enhanced diffusion. At the second stage, the irradiated material is annealed at a temperature which deletes material hardening caused by neutron irradiation and leads to P dissociation from the intragranular interphase boundaries, but, at the same time, does not lead to P dissociation from GBs. For the WWER-1000 RPV materials, this annealing temperature $T_{anneal} = 450^{\circ}C$ [7]. In addition, for the effective P diffusion coefficient to be determined, thermal aging should be carried out at the temper brittleness temperature [7].

According to the [7] time dependence of transition temperature shift due to P thermal aging, ΔT_k (t) is determined on the basis of the following considerations. The dependence ΔT_k (t) has been deducted when using the McLean equation [6], the theory of radiation-induced diffusion [11–22], and the introduced relation between the transition temperature T_k and P concentration on the interphase boundaries and/or GBs at the current moment of time (C_p^t) [7]. The transition temperature is taken as the temperature at which the Charpy impact strength equals 47 J or fracture toughness for specimens with thickness of 25 mm equals 100 MPam$^{1/2}$ for the fracture probability of 50%.

The McLean equation is presented in the form

$$\left(C_p^t - C_p^0\right) = \left(C_p^\infty - C_p^0\right) \cdot \left[1 - \exp\left(\frac{4D_p t}{\gamma^2 d^2}\right)\mathrm{erfc}\left(\frac{2\sqrt{D_p t}}{\gamma d}\right)\right], \quad (1)$$

where C_p^0, C_p^t, and C_p^∞ are the P concentrations at the interfaces and/or GBs at the given temperature at the initial moment of time ($t = 0$), at the time t, and at $t = \infty$, respectively; D_P is the P diffusion coefficient in general depending on temperature and neutron flux (neutron dose rate) [14]; d is the GB thickness; $\gamma = C_p^\infty / C_p^v$ where C_p^v is the bulk P concentration in atomic percentage.

The relation between T_k and C_p^t takes into account possible P segregations in the material in the initial condition and after thermal aging during time t. It is taken in the form [7].

$$T_k = \alpha + \beta \cdot C_p^t, \quad (2)$$

where α and β are some material constants.

Based on (1) and (2), the dependence ΔT_k (t) is presented in the form [7]:

$$\Delta T_k = \left(T_k^\infty - T_{k0}\right) \cdot \left[1 - \exp\left(4D_{eff} \cdot t\right)\mathrm{erfc}\left(2\sqrt{D_{eff} \cdot t}\right)\right], \quad (3)$$

where T_k^∞ is the value of T_k at $t = \infty$; T_{k0} is the value of T_k in the initial condition; and D_{eff} is the effective diffusion coefficient, $D_{eff} = D_P/\gamma^2 d^2$.

Under irradiation, the P diffusion coefficient of an element (e.g., phosphorus) is calculated taking into account the production and recombination of vacancies and interstitial atoms, annihilation of point defects on the various sinks, mainly dislocations (for more details, see Section 3). In case of no irradiation, the temperature dependence of P diffusion coefficient is calculated by the well-known equation in [3] similar to the Arrhenius equation.

After the material two-phase treatment (irradiation + annealing), the value of transition temperature T_k is determined for this material. Knowing T_{k0}, the value of T_k for material condition after postirradiation annealing and value of D_{eff} under irradiation, the value of T_k^∞ corresponding to the RPV operation temperature is determined from (3) where $\Delta T_k = T_k - T_{k0}$. The dependence ΔT_k (t) for unirradiated material is calculated by (3) on the basis of determined value of T_k^∞ and calculated value of D_{eff} for $T = T_{oper}$ when there is no irradiation [7].

So, the main idea of the method proposed in [7] is the formation of the grain boundaries P segregation during short-term irradiation due to strong acceleration of P diffusion under neutron irradiation at operation temperature of RPV. Strong acceleration of P diffusion under neutron irradiation up to now has not been proved directly. At the same time, there are some indirect proofs. In particular, it is well known that neutron irradiation leads to significant increase in the vacancies and interstitials concentrations and, as a result, to significant increase in the self-diffusion coefficient [11–22]. Experimental studies [10, 28] have also revealed that P segregations can be formed under neutron irradiation at sufficiently low temperature ($T = 50^{\circ}C$) when thermodiffusion of phosphorus is very small.

Phosphorus is subsized element (atomic radius of P is less than Fe radius); therefore, P diffusion may occur by both vacancy and interstitial mechanisms. Hence, it may be expected that an increase in the vacancies and interstitials concentrations under irradiation may increase equally both the self-diffusion coefficient and P diffusion coefficient. At present, there are only theoretical justifications for this consideration [8, 9, 11–14]; however, experimental data proving it are absent.

The aim of the present work is to obtain experimental data showing strong influence of neutron irradiation on P diffusion, that is, to prove that neutron irradiation increases equally both the self-diffusion coefficient and P diffusion coefficient.

2. Statement of the Problem

The effect of temperature on P diffusion and equilibrium P segregation at GBs has been studied well enough by now [3, 6, 29]. The formation of P segregations at GBs leads to intergranular brittle fracture (IBF) [2, 3, 19, 29]. With a higher P concentration at GBs, the portion of IBF increases. According to (1), the P concentration at GBs is determined by the product $D_{\text{eff}} \cdot t$. Hence, the portion of IBF is controlled by the product $D_{\text{eff}} \cdot t$. Then, if the basic consideration of the new method is true and the condition $D^{\text{T}}_{\text{eff}} \cdot t^{\text{T}} \approx D^{\text{F}}_{\text{eff}} \cdot t^{\text{F}}$ is met, the portion of IBF (when the nonhardening brittle fracture mechanism occurs) should be approximately the same both for thermally aged material and material after neutron irradiation and annealing. In the above condition, $D^{\text{T}}_{\text{eff}}$ is the effective thermal diffusion coefficient of phosphorus, t^{T} is the exposure time at a higher temperature, $D^{\text{F}}_{\text{eff}}$ is the effective diffusion coefficient of phosphorus under neutron irradiation, and t^{F} is the time of neutron irradiation.

Thus, the following experimental procedure may be proposed for justification of the proposed method in [7]. Two different treatments should be carried out for the investigated material. One treatment is thermal aging and the another is two-phase treatment (irradiation + annealing). The regimes for these treatments should be those for which the condition $D^{\text{T}}_{\text{eff}} \cdot t^{\text{T}} \approx D^{\text{F}}_{\text{eff}} \cdot t^{\text{F}}$ is met. Here, the $D^{\text{F}}_{\text{eff}}$ parameter should be calculated with the assumption that neutron irradiation increases practically equally both the self-diffusion coefficient and P diffusion coefficient (i.e presented hereafter in Section 3). Postirradiation annealing allows one to exclude any influence of irradiation-induced defects on material embrittlement except for the influence of grain boundaries P segregations that is typical for thermal aging.

Specimens machined from thermally aged material and material after postirradiation annealing should be tested over brittle fracture temperature range, and SEM examination of fracture surfaces should be performed to compare the portions of IBF for these materials.

If the portions of IBF for these material conditions coincide, then it may be concluded that the aim of the present paper is reached and the method proposed in [7] for prediction of thermal embrittlement is verified.

3. Calculative Estimation of the P Diffusion Coefficient under Neutron Irradiation

Radiation-enhanced diffusion coefficients of self-diffusion (hereinafter Fe atoms) D_{Fe} and impurity atoms (hereinafter P atoms) D_{p} can be written neglecting the correlation factors as follows [8, 9, 33]:

$$D_{\text{Fe}} = d_{\text{v}}C_{\text{v}} + d_{\text{i}}C_{\text{i}} \approx 2d_{\text{v}}C_{\text{v}}, \tag{4}$$

$$\begin{aligned} D_{\text{p}} &= \xi_{\text{pv}}d_{\text{pv}}C_{\text{v}} + \xi_{\text{pi}}d_{\text{pi}}C_{\text{i}} \\ &= \xi_{\text{v}}d_{\text{v}}C_{\text{v}} + \xi_{\text{i}}d_{\text{i}}C_{\text{i}} \approx (\xi_{\text{v}} + \xi_{\text{i}})d_{\text{v}}C_{\text{v}} \approx \xi_{\text{p}}d_{\text{v}}C_{\text{v}}, \end{aligned} \tag{5}$$

where C_{v} and C_{i} are the average vacancy and interstitial concentrations in the bulk depending on the point defect (PD) generation rate and sink density, d_{n} and d_{pn} ($n = \text{v}, \text{i}$) are the Fe and P diffusivities via vacancy and interstitial mechanisms, ξ_{pn} accounts for the binding energies E^{b}_{pn} of P atoms with PD as $\xi_{\text{pn}} = \exp(E^{\text{b}}_{\text{pn}}/kT)$, ξ_{n} accounts additionally for the difference in migration energies of Fe $E^{\text{m}}_{\text{Fen}}$ and P E^{m}_{pn} atoms: $\xi_{\text{n}} = \exp(E^{\text{b}}_{\text{pn}} + (E^{\text{m}}_{\text{Fen}} - E^{\text{m}}_{\text{pn}})/kT) = \exp(E^{\text{b}}_{\text{neff}}/kT)$, and $\xi_{\text{p}} = \exp(E^{\text{b}}_{\text{eff}}/kT)$, where $E^{\text{b}}_{\text{eff}}$ is some effective binding energy. The equality $d_{\text{v}}C_{\text{v}} \approx d_{\text{i}}C_{\text{i}}$ corresponding to steady irradiation [33] was used in (4) and (5).

Neglecting the thermal equilibrium concentration at the irradiation temperature, one can write for the average vacancy concentration [8, 9, 33]:

$$C_{\text{v}} = 0.5\left[\sqrt{\frac{4\varepsilon K}{\mu_{\text{R}}d_{\text{v}}} + \left(\frac{\rho_{\text{s}}}{\mu_{\text{R}}}\right)^2} - \frac{\rho_{\text{s}}}{\mu_{\text{R}}}\right], \tag{6}$$

where K is the PD production rate, ρ_{s} is the PD sink strength, μ_{R} is the recombination coefficient accounting for PD recombination at the rate $\mu_{\text{R}}d_{\text{i}}C_{\text{i}}C_{\text{v}}$, and ε is the cascade efficiency in producing freely migrating PD (usually in the range $0.1 \div 1$).

Equation (6) can be rewritten as follows:

$$C_{\text{v}} = \frac{\varepsilon \text{K}}{\rho_{\text{s}}d_{\text{v}}} \cdot \frac{2}{1 + \sqrt{1 + Q}}, \tag{7}$$

where the parameter $Q = 4\varepsilon K\mu_{\text{R}}/d_{\text{v}}\rho_{\text{s}}^2$.

We can consider two limiting cases:

(1) PD sinks are dominated or d_{v} is high, $Q \ll 1$. Then

$$C_{\text{v}} \approx \frac{\varepsilon \text{K}}{\rho_{\text{s}}d_{\text{v}}}, \tag{8}$$

(2) PD recombination is dominated or d_{v} is low, $Q \gg 1$. Then

$$C_{\text{v}} \approx \sqrt{\frac{\varepsilon \text{K}}{\mu_{\text{R}}d_{\text{v}}}}, \tag{9}$$

Substituting these concentrations in (4) and (5) one can obtain the following estimates of the above two cases: for $Q \ll 1$,

$$D_{\mathrm{Fe1}} = \frac{\varepsilon K}{\rho_s},$$
$$D_{\mathrm{Fe2}} = \sqrt{\frac{\varepsilon K d_{v0}}{\mu_R}} \exp\left(\frac{-E^m_{\mathrm{Fev}}}{2kT}\right), \quad (10)$$

and for $Q \gg 1$

$$D_{\mathrm{P1}} = \frac{\varepsilon K}{\rho_s} \exp\left(\frac{E^b_{\mathrm{eff}}}{kT}\right),$$
$$D_{\mathrm{P2}} = \sqrt{\frac{\varepsilon K d_{v0}}{\mu_R}} \exp\left(\frac{2E^b_{\mathrm{eff}} - E^m_{\mathrm{Fev}}}{2kT}\right), \quad (11)$$

where d_{v0} is the preexponential factor of vacancy diffusivity d_v.

It is seen from (10) and (11) that D_{Fe1} and D_{P1} do not depend on d_v and D_{P1} decreases with increasing temperature whereas D_{P2} can increase if $2E^b_{\mathrm{eff}} < E^m_{\mathrm{Fev}}$.

Here, we adopt the following parameters: $K = 6 \times 10^{-8}$ dPa/sec for a neutron flux of 6.07×10^{17} n/m^2·s from the relation 1 dPa per 10^{25} n/m^2 ($E > 0.5$ MeV), $\varepsilon = 0.1$ for neutron irradiation [33], $d_v = 2 \times 10^{-4}$ exp $(-1.3\ \mathrm{eV}/kT)$ m^2/s from [11], $\mu_R = 8{\cdot}10^{20}$ m^{-2} (assuming recombination volume on the order of 100 lattice parameter), and $E^b_{\mathrm{eff}} = 0.3$ eV as an effective binding energy of mixed Fe–P dumbbells [33]. The ρ_s is taken to be equal to the dislocation density for RPV steel in initial condition. The ρ_s may be assumed to be equal to 10^{14} m^{-2} [7].

Then taking into account (5) and (6) for irradiation at $T \approx 300$°C, we obtain $D_p = 1.95 \times 10^{-20}$ m^2/sec. This value was used above for calculation of D^F_{eff} in Table 3 accounting for $d^2\gamma^2 = 4.54 \times 10^{-13}$ m^2 [7].

Taking into account that not much is known on the diffusion parameters of self-diffusion and P diffusion in RPV steels, justification of the above parameters is based on the following analysis.

The values taken for our estimations are following values: E^m_{Fen}=1.24 eV and $E^b_{\mathrm{pi}} = 0.17$ eV (binding energy of mixed Fe–P dumbbells) and $E^b_{\mathrm{pn}} \approx 0.3$ eV that were used in [34, 35] for modelling of P accumulation at GBs in dilute Fe–P alloys. The models were applied successfully to fit experimental data on P accumulation at GBs in RPVs at a dose of 0.01 dPa. Modelling of P accumulation at GBs in Fe–Ni–P alloys was performed [8, 9] taking into account radiation-enhanced P diffusion via both vacancy and interstitial mechanisms, radiation-induced segregation in the matrix near GBs and the Gibbsian adsorption at GBs. Vacancy migration energies in the range from 0.6 eV to 1.2 eV, interstitial migration energies from 0.1 eV to 0.30 eV, and binding energies between a P atom and an interstitial from 0.3 eV to 0.15 eV were considered. Later on, this model was applied successfully to fit experimental surveillance data for several units of WWER-440 [36] where radiation embrittlement enhancement has been observed at neutron fluences above $(2\text{-}3) \times 10^{24}$ n/m^2.

In recent years, much attention has been paid to modelling of self-diffusion and P diffusion in Fe and dilute Fe–P alloys. Molecular dynamics, ab initio, and kinetic Monte Carlo calculations are applied to elucidate the mechanisms and diffusion parameters [37–41]. Ab initio calculations reveal relatively high binding energies between P atoms and vacancies (vacancy drag effect) and very high binding energies of mixed Fe–P dumbbells on the order of 1 eV and their high mobility. In addition, a new mechanism of P atoms mobility via octahedral positions in the lattice was found as a result of interaction of a self-interstitial atom with a substitutional P atom. Formation energies and diffusivities of both mobile states are similar. However, attempts to use these diffusion parameters to fit experimental data at GB phosphorus accumulation in RPVs fail to succeed. Atomic transport via interstitials in dilute Fe–P alloys was used for modelling of GB phosphorus accumulation in RPVs [38] as applied to experimental data considered before [34, 35]. The predictions highly overestimate the data. The authors suppose that a significant portion of P atoms is trapped in stable two-P complexes or segregated on point defect clusters. Both vacancy and interstitial (via mixed Fe–P dumbbells and via octahedral positions) diffusion of P atoms were used [39, 41] to fit some experimental data on GB phosphorus accumulation in RPVs at neutron fluences up to 10^{24} n/m^2. For fitting the data, an unreally high PD sink strength of 2×10^{18} m^{-2} was adopted in calculations. Possibly, reliable data on self-diffusion and P diffusion in RPVs could be obtained in molecular dynamics modelling accounting for all most important alloying and impurity elements.

Table 1: Chemical composition of 2Cr–Ni–Mo–V steel under investigation.

Mass fraction of chemical elements (%)									
C	Si	Mn	Cr	Ni	Mo	V	S	P	Cu
0.19	0.33	0.47	2.10	1.15	0.47	0.10	0.018	0.017	0.16

4. Material, Conditions, and Results of Experiment

The material selected for investigations (2Cr–Ni–Mo–V steel) used for WWER-1000 RPVs was similar to those used previously in [7]. The chemical composition of this steel is given in Table 1. The transition temperature in the initial condition T_{k0} is equal to −5°C, yield strength (σ_Y) at $T = 20$°C is equal to 585 MPa. Several sets of Charpy specimens from the above steel were machined.

On the basis of equation describing the temperature effect on D_P [3] and estimation of D_P under neutron irradiation presented above, the following regimes of neutron irradiation and thermal aging were specified to provide the condition $D^T_{\mathrm{eff}} \cdot t^T \approx D^F_{\mathrm{eff}} \cdot t^F$. Charpy specimens were subjected to neutron irradiation in the research WWR-M reactor (St. Petersburg Institute of Nuclear Physics by B. P. Konstantinov of NRC "Kurchatov Institute") at the irradiation temperature $T \approx 300$°C with a neutron flux of 6.07×10^{17} n/m^2·s for ≈1000 hours. Then, the specimens were divided into two sets. The first set was investigated in the irradiated condition, the second set was annealed at $T = 450$°C for $t = 50$ and for 100 hours.

The temperature dependence of impact strength was determined for each from two sets on the basis of impact tests.

Table 2: Material conditions, mechanical properties, and the portion for IBF of 2Cr–Ni–Mo–V steel.

Material condition	T (°C)	Exposure time (hrs)	ΔT_k (°C)	$\Delta\sigma_Y$ at 20°C (MPa)	IBF portion (%)
Initial condition	—	—	—	—	1-2
Thermal aging	500	10	6	—	5–7
Thermal aging	500	1000	31	—	70–80
Irradiation $F \approx 2 \times 10^{24}$ n/m^2	300	1000	185	260	10–12
Irradiation + annealing	450	50	35	−5	40–50
Irradiation + annealing	450	100	32	—	65–75
Initial condition + annealing	450	50	0	0	1-2
Initial condition + annealing	450	100	—	—	4–6

Note. $\Delta T_k = T_k - T_{k0}$; $\Delta\sigma_Y = \sigma_Y - \sigma_{Y0}$, where T_k and σ_Y are values for considered material condition; T_{k0} and σ_{Y0} are values for material in initial condition.

Thermal aging was conducted at a temperature of 500°C with exposures for 10 and 1000 hours. The temperature of thermal aging was taken to be equal to the temperature leading to the maximum degree of embrittlement with isothermal exposures of the same duration. After each exposure (10 and 1000 hours), the set of specimens was taken out from the furnace and impact tested with determining T_k.

Additionally, the steel in initial condition was annealed at $T = 450$°C for $t = 50$ and 100 hours. Such material condition was investigated to compare the fracture modes after annealing of irradiated material and material in initial condition.

For steel in the irradiated condition and that after irradiation and annealing, tension tests were performed at the temperature $T = 20$°C using cylindrical specimens 3 mm in diameter and 15 mm in the gouge length. Tensile specimens were machined from the halves of broken Charpy specimens.

Some broken Charpy specimens from each tested set were investigated by SEM. Additionally, SEM investigation was applied to broken specimens from steel in the initial condition subjected to annealing.

All SEM investigations were made on the scanning electron microscope Hitachi™ 3000 placed in the "hot cell" in the laboratory of CRISM "Prometey."

The results of mechanical tests and SEM investigations are presented in Table 2, Figures 1 and 2. As can be seen from Table 2, after thermal aging with an exposure for 1000 hours, the portion of intergranular brittle fracture achieves 80%.

Neutron irradiation results in the intensive material embrittlement ($\Delta T_k = 185$°C), even though, the portion of IBF is insignificant and fails to exceed 12% (Table 2, Figure 2). After annealing, the degree of material embrittlement decreases (Table 2) but, at the same time, the portion of IBF increases. This phenomenon will be explained in the following section.

It should be noted that annealing of the steel in the initial condition at a temperature of 450°C does not result in significant increase in IBF (Table 2). It means that neutron irradiation, but not annealing, results in significant increase in P concentrations on GBs and hence, significant increase of the portion of IBF.

Based on the results obtained for ΔT_k and corresponding exposure time, the values of T_k^∞ and D_{eff} were calculated for material under aging at $T = 500$°C and T_k^∞ was calculated for material under irradiation at $T = 300$°C according to the method proposed in [7]. Calculations of D_{eff} under irradiation are presented below (Section 3). Table 3 presents the calculated values of T_k^∞ and $D_{eff} \cdot t$ for different material conditions. Also, Table 3 gives the value of $D_{eff} \cdot t$ calculated at a temperature of 300°C.

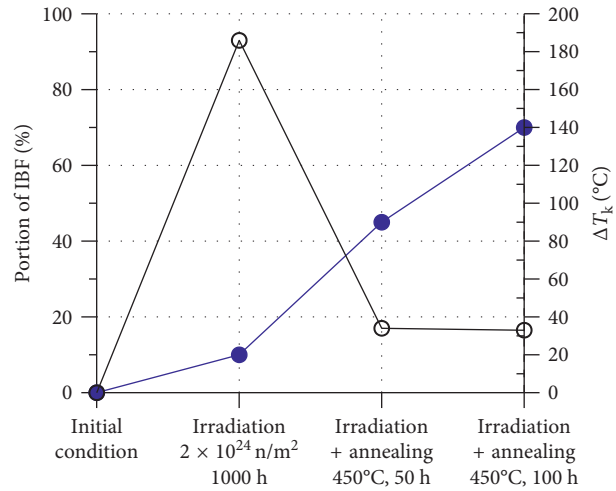

Figure 1: The portion of IBF and the ΔT_k value for different conditions of 2Cr–Ni–Mo–V steel: ●, portion of IBF; ○-ΔT_k, °C.

5. Discussion

The presented experimental data show that the portion of IBF after irradiation does not exceed 12% and after post-irradiation annealing, it reaches 70% (Figure 1) though embrittlement degree for annealed material is much less than for irradiated material. Before comparing the portion of IBF of irradiated and thermally aged material, it is essential to understand the cause of a significant difference in the fracture modes for irradiated condition and that after postirradiation annealing. Relying on the referenced work [26], this result can be explained from the diagram presented in Figure 3.

For polycrystalline, metal grain boundary may be schematized as narrow zone with extremely damaged lattice [43] that results in three consequences. Firstly, it is very difficult to nucleate atomically sharp intercrystalline microcrack as damaged lattice results in microcrack tip blunting. Secondly, the anisotropy of grains gives rise to additional shear stresses acting along GBs. Therefore, the intercrystalline

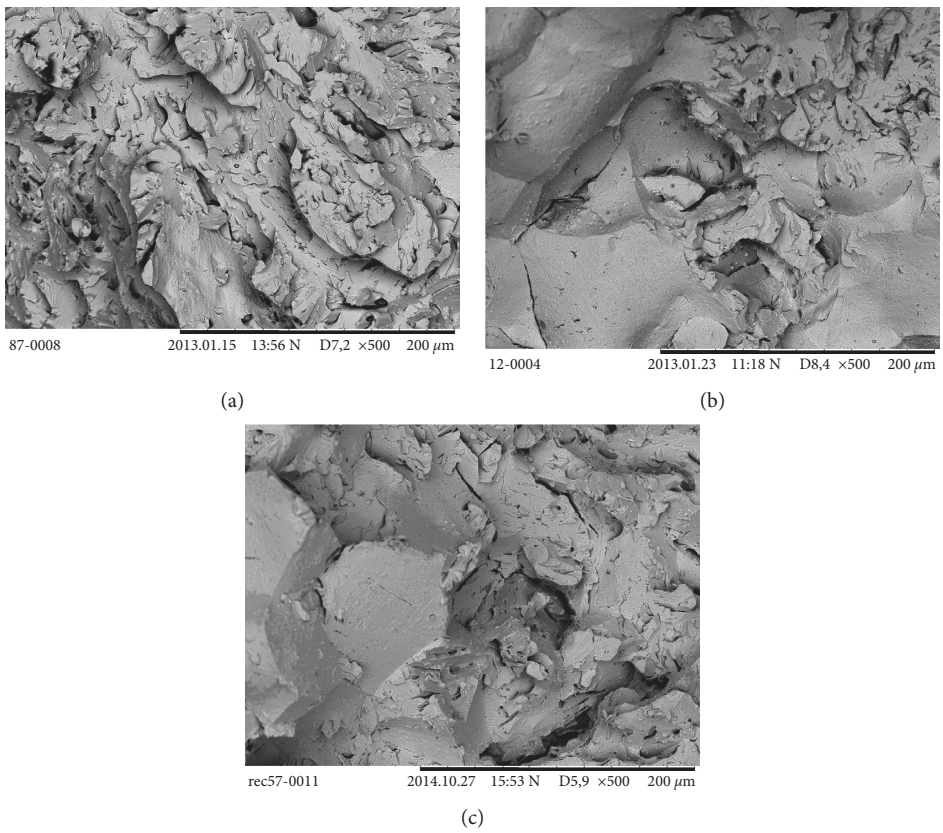

Figure 2: Typical fracture surfaces of broken Charpy specimens from 2Cr–Ni–Mo–V steel in (a) initial condition, (b) after thermal aging at 500°C for 1000 hours, and (c) after postirradiation annealing at 450°C for 100 hours.

Table 3: $D_{\text{eff}} \cdot t$ and T_k^{∞} values for different conditions of 2Cr–Ni–Mo–V.

Conditions	Temperature, °C	Time, hrs	Effective diffusion coefficient, sec^{-1}	$D_{\text{eff}} \cdot t$	T_k^{∞}, °C
Neutron irradiation	300	1000	$4.25 \cdot 10^{-8}$	0.15	58
Thermal aging	500	1000	$5.49 \cdot 10^{-8}$	0.19	55
Thermal aging	300	1000	$4.48 \cdot 10^{-14}$	$0.16 \cdot 10^{-6}$	—

microcrack blunting due to dislocation emission from its tip becomes more probable than for a transgranular microcrack. Thirdly, propagation of intercrystalline microcrack is practically impossible without dislocation emission from its tip (in contrast to transcrystalline microcrack which may propagate on cleavage plane without dislocation emission) that requires large expenditure of energy. Therefore, for unirradiated steels, it may be taken that the resistance to nucleation and propogation of transcrystalline microcrack is less than the resistance to intercrystalline microcrack.

Thus, for material in the initial condition, resistance of transgranular brittle fracture (TBF) is lower than the resistance of IBF. Therefore, material in the initial condition is mainly fractured by transgranular mode. Neutron irradiation leads to the formation of point defects, dislocation loops, precipitates and also leads to the formation of P segregations on the intragranular interphase boundaries and GBs. Microcracks resulting in brittle fracture cannot be nucleated on point defects, dislocation loops, and precipitates as these microcracks are much larger than sizes of these radiation defects [26, 27]. Therefore, the role of these radiation defects is hardening of material (increase of σ_Y) that results in embrittlement due to increase of stresses near notch or crack tip in specimen. P segregations caused by irradiation decrease the resistance to nucleation of both transgranular and intergranular microcracks and also decrease the resistance to intergranular microcracks propagation due to the weakening of atomic bonds [10, 19, 23, 26, 36]. Hardening of material and intragranular and intergranular P segregations results in strong decrease of both TBF and IBF resistance in such manner that TBF resistance is lower than IBF. Thus, a degree of material embrittlement increases strongly (Figure 1), but the fracture mode remains similar to material in initial condition. Therefore, irradiated material is mainly fractured by transgranular mode as well as material in the initial condition.

Another situation is observed for brittle fracture of steels annealed after irradiation. It is shown [42, 44] that temperature for dissociation of P segregations in a grain is less than temperature for dissociation of grain boundary

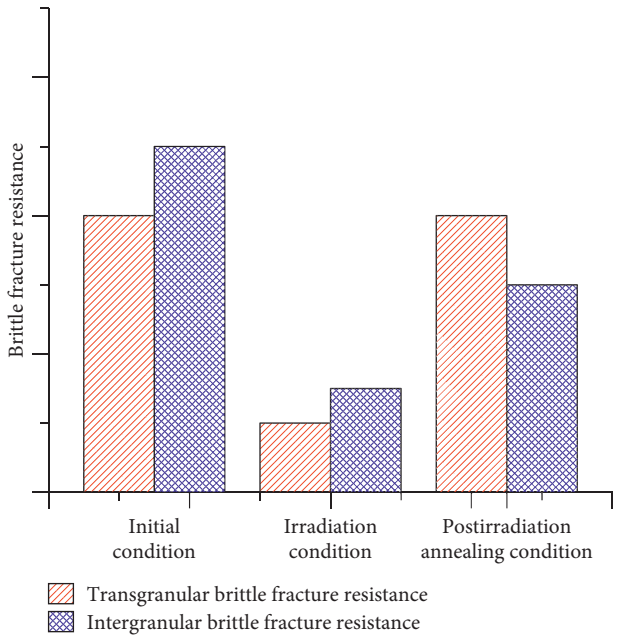

FIGURE 3: Schematic representation of brittle fracture resistance for 2Cr–Ni–Mo–V steel in three conditions: initial condition, irradiation condition, and postirradiation annealing condition.

P segregations. As shown in [42, 44], dissociation of P segregations in a grain begins at temperature $T \approx 450^{\circ}$C. At the same time, temperature for dissociation of grain boundary P segregations is approximately equal to 600–650°C [42, 45–47]. Thus, it has become clear that under annealing at $T_{ann} = 450^{\circ}$C, P segregations dissociate in a grain only, and grain boundary P segregations do not dissociate.

Yield strength of annealed material is fully recovered (see Table 2). As a result, both TBF resistance and IBF resistance increase. TBF resistance is fully recovered up to value corresponding material in initial condition. IBF resistance is recovered partially, as intergranular P segregations do not dissociate.

Thus, the relation of transgranular and intergranular brittle fracture resistance is changed that leads to fracture mainly on GBs. As the minimum brittle fracture resistance for material after annealing is less than for material in initial condition, only the partial recovery of material embrittlement occurs that is a characterized residual value of ΔT_k (see Figure 1). This ΔT_k is connected with intergranular P segregations only.

Thus, the portion of IBF does not always correlates univocally with the degree of material embrittlement. With increase of IBF portion ΔT_k may decrease.

Since the subject of interest is phosphorus diffusion, that is, the process leading to the nonhardening mechanism of material embrittlement, the comparison should be made for material conditions when the hardening mechanism is excluded. Therefore, two material conditions are considered: after thermal aging and after postirradiation annealing.

SEM investigations (Table 2, Figure 2) show that the portion of IBF after thermal aging achieves 80%. After postirradiation annealing, it makes up 70%. These results allow the conclusion to be made that intergranular P concentration for both material conditions is nearly the same.

A similar conclusion follows from the calculations presented in Table 3. Indeed, parameter controlling accumulation of P in GBs under irradiation $D_{eff}^{F} \cdot t^{F} = 0.15$ is close to parameter $D_{eff}^{T} \cdot t^{T} = 0.19$ for thermal diffusion of P. So, the condition $D_{eff}^{T} \cdot t^{T} \approx D_{eff}^{F} \cdot t^{F}$ is met.

Thus, the predictions obtained are in close agreement with the results of SEM investigations. So, the estimated values of the effective diffusion phosphorus coefficient under neutron irradiation are supported experimentally. Really, neutron irradiation increases the P diffusion coefficient by some orders. The last row of Table 3 includes the value of $D_{eff} \cdot t$ with no influence of neutron irradiation, that is, only due to thermal action at the RPV operation temperature. It can be seen that the values of $D_{eff} \cdot t$ in the first and the third rows of Table 3 are different by some orders that points to a very strong effect of neutron irradiation on the P diffusion coefficient. The results obtained have shown that neutron irradiation affects practically equally the self-diffusion coefficient and P diffusion coefficient.

So, the obtained experimental results and performed calculative estimation allow one to conclude that the proposed method [7] may be used for prediction of long-term thermal embrittlement on the basis of test results for material annealed after short-term neutron irradiation.

6. Conclusions

(1) 2Cr–Ni–Mo–V steel has been investigated in different conditions, namely, in initial conditions, after thermal aging at 500°C, after neutron irradiation at 300°C, after postirradiation annealing, and after annealing of the steel in initial condition. On the basis of impact strength tests results, the effect of different treatments (thermal aging, irradiation, and annealing) on degree of material embrittlement has been determined in terms of the transition temperature of brittleness. For each material condition, SEM investigation has been carried out and intergranular brittle fracture portion has been determined.

(2) On the basis of performed investigations, the method using the test results of irradiated and annealed specimens has been verified that was proposed for prediction of long-term embrittlement of RPV steels (in terms of the transition temperature) caused by P segregation.

(3) A strong effect of neutron irradiation on the P diffusion coefficient has been verified experimentally. The effect of neutron irradiation on the self-diffusion coefficient and on the P diffusion coefficient is nearly the same.

(4) It is shown that postirradiation annealing considerably decreases the degree of material embrittlement in terms of transition temperature; however, after annealing, the portion of intergranular brittle fracture increases. These results are explained from the physical point of view. Thus, it is possible situation when with increase of portion of intergranular brittle fracture, material toughness increases also.

Conflicts of Interest

The authors declare that there are no conflicts of interest regarding the publication of this paper.

Acknowledgments

This work was carried out in frame of Contract no. 14.595.21.0004 with the Ministry of Education and Science of Russian Federation (unique identifier RFMEFI59517X0004). Experimental investigations were performed with the facilities of the hot-laboratory "Test and technological complex for research of irradiated and radionuclide materials" and Research Center "The composition, microstructure, and properties of structural and functional materials" at NRC "Kurchatov Institute"–CRISM "Prometey."

References

[1] S. A. Arrhenius, "On the influence of carbonic acid in the air upon the temperature of the ground," *London, Edinburgh, and Dublin Philosophical Magazine and Journal of Science*, vol. 41, no. 251, pp. 237–276, 1896.

[2] Y. I. Ustinovshchikov and O. A. Bannikh, *Nature of Temper Brittleness of Steel*, Nauka, Moscow, 1984, in Russian.

[3] L. M. Utevsky, E. J. Glikman, and G. S. Kark, *Reversible Temper Embrittlement of Steel and Iron Alloys*, Metallurgiya, Moscow, 1987, in Russian.

[4] J. H. Hollomon and L. D. Jaffe, "Time-temperature relations in tempering steel," *Transactions of the American Institute of Mining and Metallurgical Engineers*, vol. 162, pp. 223–249, 1945.

[5] Russian Standard (Guide), *Standard for Strength Calculation of Equipments and Pipelines of Nuclear Power Plants*PNAE G-7-002-86, p. 525, Energoatomizdat, 1989, in Russian.

[6] D. McLean, *Grain Boundaries in Metals*, Oxford University Press, London, UK, 1957.

[7] B. Z. Margolin, E. V. Yurchenko, A. M. Morozov, and D. A. Chistyakov, "Prediction of the effects of thermal ageing on the embrittlement of reactor pressure vessel steels," *Journal of Nuclear Materials*, vol. 447, no. 1–3, pp. 107–114, 2014.

[8] I. A. Stepanov, V. A. Pechenkin, and Y. V. Konobeev, "The modeling of radiation-induced phosphorus segregation at point defect sinks in dilute Fe-P alloys," in *Effects of Radiation on Materials: 21st International Symposium, ASTM STP 1447*, pp. 579–589, ASTM International, West Conshohocken, PA, USA, 2004.

[9] V. A. Pechenkin, I. A. Stepanov, and Y. V. Konobeev, "Modelling of phosphorus accumulation on grain boundaries in iron alloys under irradiation," in *Effects of Radiation on Materials: 20th International Symposium, ASTM STP 1405*, pp. 174–187, ASTM International, West Conshohocken, PA, USA, 2001.

[10] N. N. Alekseenko, A. D. Amaev, I. V. Gorynin, and V. A. Nikolaev, *Radiation Damage of Nuclear Power Plant Pressure Vessel Steels*, American Nuclear Society, La Grange Park, IL, USA, 1997.

[11] G. S. Kark, "The role of radiation enhanced diffusion of impurities in the embrittlement of pearlitic steel under neutron irradiation," Metal science and heat treatment of steels for equipment of power plants, in Proceedings of the CNIITMASH, Moscow, Russia, 1983, in Russian.

[12] A. M. Shalaev, *Radiation-Enhanced Diffusion in Metals*, Atomizdat, Moscow, 1972, in Russian.

[13] G. J. Dienes and A. C. J. Damask, "Radiation enhanced diffusion in solids," *Journal of Applied Physics*, vol. 29, no. 12, pp. 1713–1721, 1958.

[14] G. J. Dienes and G. H. Vineyard, *Radiation Effects in Solids*, Interscience Publishers, New York, NY, USA, 1957.

[15] D. Heitkamp and W. Biermann, "Effect of alpha bombardment on the diffusion of lead in silver," *Acta Materialia*, vol. 14, no. 10, pp. 1201–1212, 1966.

[16] P. R. Okamoto and L. E. Rehn, "Radiation-induced segregation in binary and ternary alloys," *Journal of Nuclear Materials*, vol. 83, no. 1, pp. 2–23, 1979.

[17] P. J. E. Bischler and R. K. Wild, "A microstructural study of P segregation and intergranular fracture in neutron irradiated submerged-arc weld," in *Effects of Radiation on Materials: 17th International Symposium, ASTM STP 1270*, pp. 260–273, ASTM International, West Conshohocken, PA, USA, 1996.

[18] R. J. McElroy, C. A. English, A. J. Foreman et al., "Temper embrittlement, irradiation induced P segregation and implications for post-irradiation annealing of reactor pressure vessels," in *Effects of Radiation on Materials: 18th International Symposium (ASTM STP1325)*, pp. 296–316, ASTM International, West Conshohocken, PA, USA, 1999.

[19] B. A. Gurovich, E. A. Kuleshova, Y. I. Shtorombakh, O. O. Zabusov, and E. A. Krasikov, "Intergranular and intragranular P segregation in Russian pressure vessel steels due to neutron irradiation," *Journal of Nuclear Materials*, vol. 279, pp. 259–272, 2000.

[20] A. Kimura, M. Shibata, R. Kasada, K. Fujii, K. Fukuya, and H. Nakata, "Assessment of Neutron irradiation-induced grain boundary embrittlement by phosphorous segregation in a reactor pressure vessel steel," *Journal of ASTM International*, vol. 2, no. 3, article 12398, 2005.

[21] Y. Nishiyama, K. Onizawa, M. Suzuki et al., "Effects of neutron-irradiation-induced intergranular P segregation and hardening on embrittlement in reactor pressure vessel steels," *Acta Materialia*, vol. 56, pp. 4510–4521, 2008.

[22] Y. Nishiyama, M. Yamagushi, K. Onizawa, A. Iwase, and H. Matsuzawa, "Irradiation-induced grain-boundary solute segregation and its effect on ductile-to-brittle transition temperature in reactor pressure vessel steels," *Journal of ASTM International*, vol. 6, article JAI10195, p. 8, 2009.

[23] J. R. Hawthorne, "Radiation embrittlement," in *Embrittlement of Engineering Alloys*, C. Briant and S. Banerji, Eds., Academic Press, New York, NY, USA, 1983.

[24] A. Andrieu, A. Pineau, P. Joly, and F. Roch, "On Modelling of Thermal Embrittlement in PWR Steels using the Local Approach to Fracture," in *Proceedings of the Materials of 13th International Conference on Fracture*, Beijing, China, 2013.

[25] S.-G. Park, K.-H. Lee, K.-D. Min, M.-C. Kim, and B.-S. Lee, "Influence of the thermodynamic parameters on the temper embrittlement of SA508 Gr.4N Ni-Cr-Mo low alloy steel with variation of Ni, Cr and Mn contents," *Journal of Nuclear Materials*, vol. 426, pp. 1–8, 2012.

[26] B. Z. Margolin, V. A. Shvetsova, and A. G. Gulenko, "Radiation embrittlement modelling in multi-scale approach to brittle fracture of RPV steels," *International Journal of Fracture*, vol. 179, no. 1, pp. 87–108, 2013.

[27] B. Z. Margolin, V. A. Shvetsova, A. G. Gulenko, and V. I. Kostylev, "Prometey local approach to brittle fracture: development and application," *Engineering Fracture Mechanics*, vol. 75, pp. 3483–3498, 2008.

[28] V. V. Rybin and V. A. Nikolaev, "On mechanisms determining the dependence of radiation embrittlement of RPV steel on its chemical composition," *Voprosy Materialovedeniya (Material Science Issues)*, no. 1, pp. 27–54, 1995, in Russian.

[29] P. Lejcek, *Grain Boundary Segregation in Metals*, Springer, Heidelberg, Germany, 2010.

[30] B. Z. Margolin, E. V. Yurchenko, A. M. Morozov, N. E. Pirogova, and M. Brumovsky, "Analysis of a link of embrittlement mechanisms and neutron flux effect as applied to reactor pressure vessel materials of WWER," *Journal of Nuclear Materials*, vol. 434, pp. 347–356, 2013.

[31] M. K. Miller, A. A. Chernobaeva, Y. I. Shtrombakh et al., "Evolution of the nanostructure of VVER-1000 RPV materials under neutron irradiation and post irradiation annealing," *Journal of Nuclear Materials*, vol. 385, pp. 615–622, 2009.

[32] M. Miller, K. Rassell, J. Kocik, and E. Keilova, "Embrittlement of low copper VVER 440 surveillance samples neutron-irradiated to high fluences," *Journal of Nuclear Materials*, vol. 282, pp. 83–88, 2000.

[33] G. S. Was, *Fundamentals of Radiation Materials Science: Metals and Alloys*, p. 827, Springer-Verlag, New York, NY, USA, 2007.

[34] S. G. Druce, C. A. English, A. J. E. Foreman et al., "The modelling of irradiation-enhanced P segregation in neutron irradiated reactor pressure vessel submerged-arc welds," in *Effects of Radiation on Materials: 17th International Symposium*, pp. 119–137, ASTM International, West Conshohocken, PA, USA, 1996.

[35] A. V. Barashev, "Segregation of phosphorus atoms to grain boundaries in ferritic steels under neutron irradiation," *Philosophical Magazine Letters*, vol. 82, pp. 323–332, 2002.

[36] V. A. Pechenkin, Y. V. Konobeev, I. A. Stepanov, and Y. A. Nikolaev, "On the mechanism of irradiation embrittlement enhancement in reactor pressure vessel steels at high neutron fluences," in *Effects of Radiation on Materials: 21st International Symposium, ASTM STP 1447*, pp. 138–148, ASTM International, West Conshohocken, PA, USA, 2004.

[37] C. Domain and C. S. Becquart, "Diffusion of phosphorus in Fe: An ab initio study," *Physical Review B*, vol. 71, article 214109, pp. 1–13, 2005.

[38] E. Meslin, C.-C. Fu, A. Barbu, F. Gao, and F. Willaime, "Theoretical study of atomic transport via interstitials in dilute Fe-P alloys," *Physical Review B*, vol. 75, article 094303, pp. 1–8, 2007.

[39] K. Ebihara, T. Suzudo, M. Yamaguchi, and Y. Nishiyama, "Introduction of vacancy drag effect to first-principles-based rate theory model for irradiation-induced grain-boundary P segregation," *Journal of Nuclear Materials*, vol. 440, pp. 627–632, 2013.

[40] L. Messina, M. Nastar, T. Garnier, C. Domain, and P. Olsson, "Exact *ab initio* transport coefficients in bcc Fe–X (X = Cr, Cu, Mn, Ni, P, Si) dilute alloys," *Physical Review B*, vol. 90, article 104203, pp. 1–12, 2014.

[41] K. Ebihara, T. Suzudo, and M. Yamaguchi, "Modelling of Phosphorus Transport by Interstitial Dumbbell in α–Iron Using First-Principles-Based Kinetic Monte Carlo," *Materials Transactions*, vol. 58, no. 1, pp. 26–32, 2017.

[42] B. A. Gurovich, E. A. Kuleshova, Y. A. Nikolaev, and Y. I. Shtrombakh, "Assesment of relative contributions from different mechanisms to radiation embrittlement of reactor pressure vessel steels," *Journal of Nuclear Materials*, vol. 246, pp. 91–120, 1997.

[43] F. A. McClintock and A. S. Argon, *Mechanical Behavior of Materials*, Addison-Wesley, Boston, MA, USA, 1966.

[44] V. A. Nikolaev and V. V. Rybin, "Mechanisms controlling the composition influence on radiation hardening and embrittlement of iron-base alloys," in *Effect of Radiation on Materials: 17th International Symposium, ASTM STP 1270*, pp. 3–24, ASTM International, West Conshohocken, PA, USA, 1996.

[45] J. B. Rellick and C. J. McMahon, "Integranular embrittlement of iron-carbon alloys by impurities," *Metallurgical Transactions*, vol. 5, no. 11, pp. 2439–2450, 1974.

[46] M. P. Seah, "Grain boundary segregation and the T-t dependence of temper brittleness," *Acta Metallurgica*, vol. 25, no. 3, pp. 345–357, 1977.

[47] W. R. Tyson, "Kinetics of temper embrittlement," *Acta Metallurgica*, vol. 26, no. 9, pp. 1471–1478, 1978.